Primordial black hole dark matter evaporating on the neutrino floor

Roberta Calabrese [a,b], Damiano F.G. Fiorillo [a,b], Gennaro Miele [a,b,c], Stefano Morisi [a,b], Antonio Palazzo [d,e,*]

[a] *Università degli Studi di Napoli "Federico II", Complesso Univ. Monte S. Angelo, I-80126 Napoli, Italy*
[b] *INFN - Sezione di Napoli, Complesso Univ. Monte S. Angelo, I-80126 Napoli, Italy*
[c] *Scuola Superiore Meridionale, Università di Napoli Federico II, Largo San Marcellino 10, 80138 Napoli, Italy*
[d] *Dipartimento Interateneo di Fisica "Michelangelo Merlin", Università degli Studi di Bari, Via G. Amendola 173, I-70126 Bari, Italy*
[e] *Istituto Nazionale di Fisica Nucleare, Sezione di Bari, Via Orabona 4, 70126 Bari, Italy*

A B S T R A C T

Primordial black holes (PBHs) hypothetically generated in the first instants of life of the Universe are potential dark matter (DM) candidates. Focusing on PBHs masses in the range $[5 \times 10^{14} - 5 \times 10^{15}]$ g, we point out that the neutrinos emitted by PBHs evaporation can interact through the coherent elastic neutrino nucleus scattering (CEνNS) producing an observable signal in multi-ton DM direct detection experiments. We show that with the high exposures envisaged for the next-generation facilities, it will be possible to set bounds on the fraction of DM composed by PBHs improving the existing neutrino limits obtained with Super-Kamiokande. We also quantify to what extent a signal originating from a small fraction of DM in the form of PBHs would modify the so-called "neutrino floor", the well-known barrier towards detection of weakly interacting massive particles (WIMPs) as the dominant DM component.

1. Introduction

The identity of dark matter (DM) is one of the most puzzling mysteries in astroparticle physics and cosmology. In spite of enormous efforts, no uncontroversial non-gravitational signal of DM has emerged so far. In this context, the detection of gravitational waves from binary black hole mergers by LIGO/Virgo [1,2] has revamped the attention [3–7] towards primordial black holes (PBHs) as DM candidates, putatively generated in the early Universe from the collapse of overdensities [8–14] (see [15–19] for reviews). The Hawking radiation [20] from PBHs can give rise to observable signals. In fact, bounds on PBHs have been obtained from X-rays [21,22], γ-rays [23–25,21,26,27], 511 keV γ-ray line [28–30], $e^{\pm}$ [31], CMB [32–34], radio signals [35–37], and heating of the interstellar medium [38,39]. The possibility to constrain PBHs using neutrinos was discussed long ago in [40–42]. More recently, limits on PBHs have been obtained in [29] exploiting the searches of the diffuse supernova neutrino background (DSNB) by Super-Kamiokande (SK) [43]. Prospective bounds from JUNO have been considered in [44].

In this Letter, we entertain a novel possibility, never addressed before in the literature, proposing to detect neutrinos from PBHs with coherent elastic neutrino nucleus scattering (CEνNS). It is only recently that CEνNS, predicted long time ago [45], has been observed by COHERENT [46]. This process involving solar, DSNB and atmospheric neutrinos, is an irreducible background [47–53] (the so-called "neutrino floor" [53]) towards discovery of WIMPs in DM direct detection experiments. Here we show that neutrinos from PBHs with masses in the range $[5 \times 10^{14}, 5 \times 10^{15}]$ g, with energy between 10 MeV and 100 MeV, emerge on top of such a background. It is then possible to set prospective bounds on the PBHs fraction f_{PBH} of DM in this mass range. As a notable byproduct, we show how the neutrino floor gets modified by a hypothetical signal from PBHs.

2. Neutrinos emitted by PBHs

A black hole is believed to quantum evaporate [20], emitting radiation akin to a hot body. For a neutral non-rotating (Schwarzschild) black hole, the Hawking temperature is given by [20,54–56]

$$k_B T_{PBH} = \frac{\hbar c^3}{8\pi G_N M_{PBH}} \simeq 1.06 \left[\frac{10^{16} g}{M_{PBH}} \right] \text{MeV}, \qquad (1)$$

where four fundamental constants appear, k_B (Boltzmann), G_N (gravitational), $\hbar$ (Planck), and c (speed of light). The differential flux per unit time of emitted particles depends on their spin. For

* Corresponding author.
E-mail address: palazzo@ba.infn.it (A. Palazzo).

spin 1/2 particles with mass negligible with respect to T_{PBH} like neutrinos, it is given by

$$\frac{d^2N_\nu}{dE_\nu dt} = \frac{1}{2\pi} \frac{\Gamma_\nu(E_\nu, M_{PBH})}{\exp[E_\nu/k_B T_{PBH}] + 1}, \qquad (2)$$

where E_ν is the neutrino energy and Γ_ν is a greybody factor [54–56]. In our analysis, we employ the publicly available `Black-Hawk` code [57] for calculating the energy spectra of the emitted neutrinos, including both the primary and secondary fluxes. In [58], it has been shown that Dirac neutrinos, having twice as many degrees of freedom as the Majorana ones, would affect the PBHs evaporation making it faster (see also [59,60]). For the PBHs masses considered in our work, the change is around $\sim 10\%$ [58]. Although the additional Dirac degrees of freedom are sterile for the electroweak interactions and not detectable in the CEνNS process, their existence can alter indirectly the emission rate of the active degrees of freedom [44]. For definiteness, we assume that neutrinos have Majorana nature. We ignore neutrino oscillations being irrelevant for the flavor-blind CEνNS process. We take into account both the contributions coming from the Galactic and extragalactic PBHs. The Galactic differential neutrino flux is given by

$$\frac{d\phi_\nu^{MW}}{dE_\nu} = \int \frac{d\Omega}{4\pi} \frac{d^2N}{dE_\nu dt} \int dl \frac{f_{PBH}\,\rho_{MW}[r(l,\psi)]}{M_{PBH}}, \qquad (3)$$

where $\rho_{MW}(r)$ is the DM density of the Milky Way (MW), r denotes the galactocentric distance

$$r(l,\psi) = \sqrt{r_\odot^2 - 2lr_\odot \cos\psi + l^2}, \qquad (4)$$

with $r_\odot$ being the distance of the Sun from the Galactic center, l the line-of-sight distance to the PBH, ψ the angle between these two directions, and Ω the solid angle under consideration. For definiteness, we employ a Navarro-Frenk-White (NFW) profile [61]

$$\rho_{MW}(r) = \rho_\odot \left[\frac{r}{r_\odot}\right]^{-1} \left[\frac{1 + r_\odot/r_s}{1 + r/r_s}\right]^2, \qquad (5)$$

where we take $\rho_\odot = 0.4\,\text{GeV}\,\text{cm}^{-3}$ for the DM density in the solar neighborhood [62–67], $r_\odot = 8.5\,\text{kpc}$, and $r_s = 20\,\text{kpc}$ for the scale radius. We have checked that our limits are rather stable if we adopt a cored MW halo as suggested in [68]. For the extragalactic component, the differential flux is [16]

$$\frac{d\phi_\nu^{EG}}{dE_\nu} = \int_{t_{min}}^{t_{max}} dt\,[1 + z(t)] \frac{f_{PBH}\rho_{DM}}{M_{PBH}} \frac{d^2N_\nu}{d\tilde{E}_\nu dt}\bigg|_{\tilde{E}_\nu = [1+z(t)]E_\nu}, \qquad (6)$$

ρ_{DM} being the average DM density of the Universe at the present epoch, as determined by Planck [69]. The time integral runs from t_{min} set to the era of matter-radiation equality to t_{max}, the minimum between the PBH lifetime and the age of the Universe. The overall neutrino flux from the sum of Galactic and extragalactic contributions is plotted in Fig. 1. The solid lines refer to the total (primary + secondary) neutrino flux, while the dotted lines refer only to the secondary neutrino flux. We see that primary neutrinos have a prominent role in the overall budget for energies above 20 MeV. The three colored lines refer to three benchmark values of M_{PBH} and f_{PBH} indicated in the legend. As it will be discussed in the next section, these values are excludable at 90% C.L. with a xenon experiment with 200 tonnes yr exposure, assuming a measurement compatible with the ordinary background. In the same plot, we represent the background which is formed from solar [70], DSNB [71] and low-energy atmospheric neutrinos [72,73]. As expected from Eq. (1), smaller PBHs masses correspond to harder spectra of the emitted neutrinos with peak located at
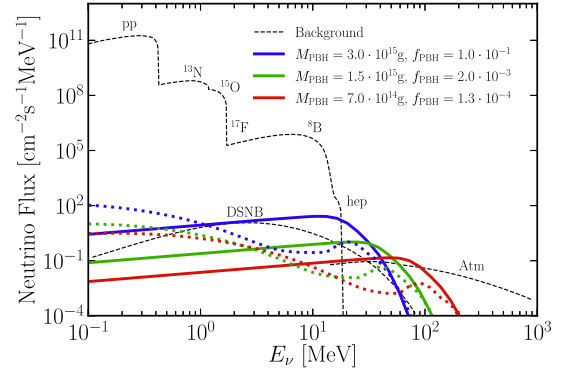

Fig. 1. Neutrino fluxes from PBHs. The black dashed contours represent the solar, DSNB and atmospheric backgrounds. The colored solid curves correspond to the total (primary plus secondary) neutrino flux from PBHs with parameters in the legend, lying on the 90% C.L. exclusion curve obtainable from a liquid xenon experiment with 200 tonnes yr exposure (black stars in Fig. 3). We also plot (dotted colored curves) the contribution to the total PBHs neutrino flux arising from secondary neutrinos.

$\sim 4.02\,T_{PBH}$ [74,75]. We see that PBHs neutrinos emerge above the abrupt fall-off of the solar *hep* neutrinos, where the dominant background is given by DSNB and atmospheric neutrinos.

3. Coherent scattering of neutrinos

Coherent elastic scattering of a neutrino ν (or antineutrino $\bar{\nu}$) on a nucleus $\mathcal{N}$ can occur if $qR \ll 1$, where $q = |\vec{q}|$ is the three-momentum transfer and R is the nuclear radius [45]. The differential cross section can be expressed as [45]

$$\frac{d\sigma_{\nu\mathcal{N}}}{dE_R}(E_\nu, E_R) = \frac{G_F^2 m_\mathcal{N}}{4\pi} Q_w^2 \left(1 - \frac{m_\mathcal{N} E_R}{2E_\nu^2}\right) F^2(q), \qquad (7)$$

where G_F is the Fermi constant, $m_\mathcal{N}$ is the nucleus mass, $Q_w = \left[N - Z(1 - 4\sin^2\theta_W)\right]$ is the weak vector nuclear charge, Z and N are the number of protons and neutrons, $\sin^2\theta_W = 0.231$ [76] is the Weinberg angle, E_R is the nucleus recoil energy, and E_ν is the neutrino energy. The recoil energy can assume the maximum value $E_R^{max} = 2E_\nu^2/(m_\mathcal{N} + 2E_\nu)$. For the nuclear form factor $F(q)$, encoding the loss of coherence for $qR > 1$, we employ the Helm parametrization [77] using the recipes provided in [78]. The differential rate of events is given by

$$\frac{dR_{\nu\mathcal{N}}}{dE_R dt} = N_T\,\epsilon(E_R) \times \int dE_\nu\,\frac{d\sigma_{\nu\mathcal{N}}}{dE_R} \frac{d\phi_\nu}{dE_\nu} \Theta(E_R^{max} - E_R), \qquad (8)$$

where N_T is the number of target nuclei in the detector, $\epsilon(E_R)$ is the detector efficiency (assumed to be equal to one), $d\phi_\nu/dE_\nu$ is the differential neutrino flux, and Θ is the Heaviside step function. In Fig. 2, we show the differential rate of events as a function of the recoil energy for the background (dashed lines), and for three benchmark values of the PBHs parameters (the same used in Fig. 1). The plots refer to an exposure of 200 tonnes yr. One can observe that the shape of the spectrum induced by PBHs neutrinos appreciably changes with the mass of the PBH. In particular, for smaller values of M_{PBH}, which correspond to more energetic neutrino fluxes, the event spectrum is similar to the atmospheric background. In contrast, for larger values of M_{PBH} with flux peaked at lower energies, the PBHs event spectrum is quite different with respect to the background. For this reason, in the statistical treatment presented in the next section we employ a binned likelihood analysis, so as to fully exploit the information contained in the spectral shape.
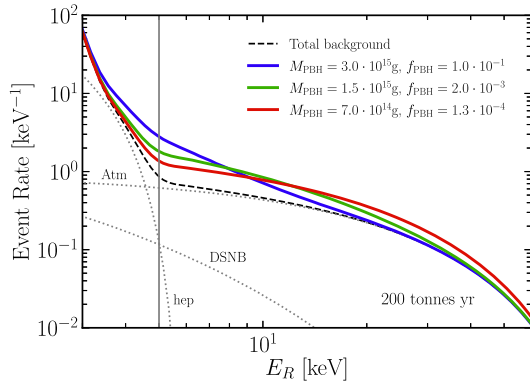
Fig. 2. Differential events rate from PBHs neutrinos. The black dashed curve is the total background from the sum of three components (each in dotted grey). The colored solid curves correspond to the event rate in the presence of PBHs neutrinos with parameters in the legend, excludable at 90% C.L. by a 200 tonnes yr xenon detector (black stars in Fig. 3). The vertical line is the threshold energy $E_R^{\text{thr}} = 5\,\text{keV}$ used in the analysis.
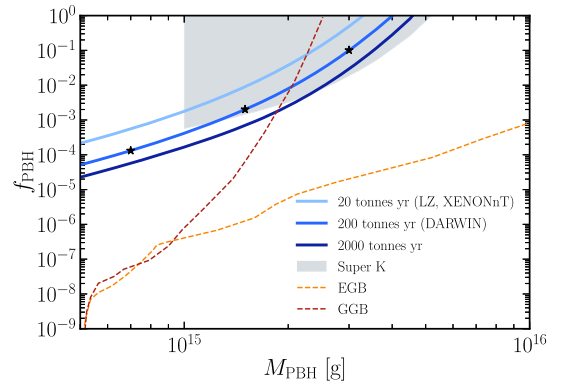

Fig. 3. Prospective upper bounds on PBHs. The exclusion contours (blue curves), all drawn at the 90% C.L. for 1 d.o.f., refer to a xenon experiment with three different exposures. Two of them correspond to the planned experiments (LZ/XENONnT and DARWIN), while the third one refers to an ideal setup. The black stars indicate the three benchmark values used for Figs. 1, 2 and 4. The shaded region represents the upper bounds obtained in [29] from the DSNB searches of SK [43]. The dashed curves represent the upper limits derived from the Galactic (GGB) and extragalactic (EGB) γ-ray background.

4. PBHs at next-generation detectors

In order to derive prospective upper limits on the fraction of DM composed of PBHs, we implement the χ^2 test statistic defined as

$$\chi^2(\boldsymbol{\theta}) = \min_{\boldsymbol{\alpha}}\Big[\chi^2(\boldsymbol{\theta}, \boldsymbol{\alpha}) + (1 - \boldsymbol{\alpha})^T \Sigma_{\boldsymbol{\alpha}}^{-1}(1 - \boldsymbol{\alpha})\Big], \quad (9)$$

where $\boldsymbol{\theta}^T = [M_{\text{PBH}}, f_{\text{PBH}}]$, and $\boldsymbol{\alpha}^T = [\alpha_1, \alpha_1, \alpha_3]$ represent respectively the vector of the model parameters and that of the nuisance parameters associated to the normalization of the three backgrounds components (solar *hep*, DSNB, atmospheric) with respect to their best theoretical estimates. The uncertainties on the backgrounds are encoded in the covariance matrix $\Sigma_{\boldsymbol{\alpha}} = \text{diag}(\sigma_{\alpha_1}^2, \sigma_{\alpha_2}^2, \sigma_{\alpha_3}^2)$, which we take diagonal because the three fluxes have independent origin. For the uncertainties, we assume 30%, 50% and 20%, respectively for solar *hep* [70], DSNB [71] and atmospheric neutrinos [72,73]. The first term in Eq. (9) is defined as

$$\chi^2(\boldsymbol{\theta}, \boldsymbol{\alpha}) = -2\ln\frac{L_0}{L_1}, \quad (10)$$

with likelihoods given by

$$L_0 = \prod_i P(x = \overline{N}_{\text{Bck}}^i; \lambda = N_{\text{PBH}}^i(\boldsymbol{\theta}) + N_{\text{Bck}}^i(\boldsymbol{\alpha})), \quad (11)$$

and

$$L_1 = \prod_i P(x = \overline{N}_{\text{Bck}}^i; \lambda = \overline{N}_{\text{Bck}}^i), \quad (12)$$

where $P(x, \lambda)$ is the Poisson distribution, i is the bin index, $\overline{N}_{\text{Bck}}^i$ is the nominal number of background events expected in the i-th bin, whereas N_{PBH}^i is the number of PBHs events, and $N_{\text{Bck}}^i = \sum_j \alpha_j \overline{N}_{\text{Bck},j}^i$ is the background, which in the fit varies with the nuisance parameters α_j's. The second contribution in Eq. (9) is a penalty term. We neglect other possible backgrounds, in particular those arising from electron recoils of solar pp and ^{7}Be neutrinos, since as shown in [79], these can be effectively suppressed through a statistical discrimination of the photon and ionization signals. In our statistical analysis, we employ ten bins in the recoil energy window [5 − 50] keV. The choice of the threshold $E_R^{\text{thr}} = 5\,\text{keV}$ is dictated by the position of the sharp cutoff of the *hep* neutrino event rate (see Fig. 2), which in this way has a marginal impact

in our results. We have checked that even multiplying by a factor of two the nominal value [71] of the DSNB as suggested by most recent theoretical evaluations [80–83], which point towards somewhat larger fluxes, the results are basically unchanged. Fig. 3 displays the 90% C.L. exclusion limits obtainable from a xenon detector with the three benchmark exposures reported in the legend. The 20 tonnes yr exposure should be attainable in LZ and XENONnT, while the higher value of 200 tonnes yr refers to the more ambitious project DARWIN. The third contour corresponds to 2000 tonnes yr, which probably may be considered as an ultimate goal for liquid xenon detectors. Such high exposures seem to be less extreme for Argon based detectors [84]. In the same plot, for comparison, we report as a shaded grey region, the upper bounds obtained in [29] from the DSNB searches of SK [43].[1] We see that an improvement of one order of magnitude is attainable with the most high exposures.

We remark that the prospective CEνNS bounds shown in Fig. 3, while improving the existing neutrino limits derived from SK, are weaker than those obtained with other probes sensitive to electromagnetic interactions, particularly from Galactic γ-ray background (GGB) and diffuse extragalactic γ-ray background (EGB) (see for example the review [16]). In Fig. 3, we report for completeness the upper limits obtained from GGB and EGB as extracted from Figure 10 of [16]. We see that for PBHs masses $M_{\text{PBH}} \gtrsim 2 \times 10^{15}$ g, the neutrino bounds are stronger than the GGB limits (red dashed curve). On the other hand, the EGB limits (orange dashed curve) are stronger than the neutrino limits over the whole range of masses we explored. We also mention the bounds from electron and positrons [31], which are quite strong in the region of PBH masses we are considering. Concerning these last bounds, one should bear in mind that they sensibly depend on the cosmic rays propagation model adopted in the theoretical calculations, which is currently subject to several uncertainties. In contrast, neutrinos travel undisturbed over Galactic and extragalactic distances and are unaffected by propagation issues. Even the uncertainties on the mass-mixing parameters are innocuous, being neutrino oscillations irrelevant for the flavor blind CEνNS process. Therefore, the prospective CEνNS bounds (and all neutrino limits in general)

---

[1] In [29], which considers both spinning and non-spinning PBHs, the upper limits are reported for masses above 10^{15} g because rotating black holes evaporate faster than the non-rotating ones and can contribute to the present DM content for $M_{\text{PBH}} \gtrsim 7 \times 10^{14}$ g. In our work, focused on non-rotating PBHs, we show the limits down to $M_{\text{PBH}} = 5 \times 10^{14}$ g, as it is customary in the literature.
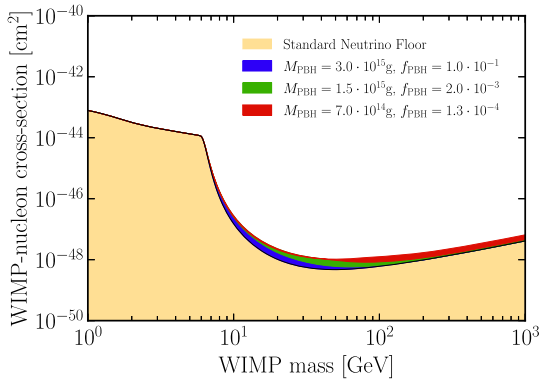
Fig. 4. Impact of PBHs on the Neutrino Floor. The black contour delimiting the yellow region represents the ordinary neutrino floor, while the upper border of the colored bands correspond to the modifications induced by neutrinos from PBHs with parameters in the legend. These benchmark values are excludable at 90% C.L. by a xenon experiment with 200 tonnes yr exposure (corresponding to the black stars in Fig. 3).

have the advantage of being very robust and are therefore highly complementary to those attainable with other messengers. We also stress that the CEνNS sensitivity could be further improved with better modeling of the atmospheric neutrinos or increasing the exposure. Also, exploiting the information on the arrival direction of neutrinos, which is different in the case of atmospheric (almost isotropic) and PBHs neutrinos (mostly pointing to the Galactic center), could allow CEνNS to gain sensitivity in the future.

5. Impact of PBHs on the neutrino floor

Neutrinos originating from the Sun, DSNB and Earth's atmosphere constitute a background in DM direct searches [47–53], giving rise to the so-called "neutrino floor" [53], an ultimate limit to the discovery potential of WIMPs. While such a limitation holds for any kind of interaction, and can be generalized to several types of WIMP-nucleus effective field theory operators [85,86], it is customary to adopt the case of spin-independent interaction as a benchmark. As a matter of fact, the experiment XENON1T [87] has almost reached the goal of detecting the solar ^{8}B neutrino background, which is dominant for WIMP masses around $m_\chi \sim 6$ GeV. The next-generation facilities with very high exposures will unavoidably encounter the neutrino floor also for larger WIMP masses, where the background from DSNB and atmospheric neutrinos is relevant. Going below such a floor will require exploiting timing structure of the signal [88], combining different targets [89], or using directional information [90–92]. Interestingly, the neutrino background can be affected by exotic neutrino interactions [93–96], with consequent modification of the standard floor [97–102], which can be influenced also by neutrinos from decay of massive particles [103,104] and supermassive black holes [105].

Here we quantify how the neutrinos from PBHs modify the floor following the prescription of [53]. For definiteness and consistency with the previous sections, we consider the case of a xenon target and adopt the same NFW profile as per Eq. (5). Following [78], we employ a Galactic Maxwell-Boltzmann velocity distribution with most probable speed $v_0 = 220$ km/s, truncated at the escape velocity $v_{esc} = 544$ km/s and boosted into the laboratory frame with $v_{lab} = 232$ km/s. For a fixed value of the WIMP mass we calculate the WIMP-nucleon cross-section $\sigma_{\chi n}$ that can be excluded at the 90% confidence level (corresponding to 2.3 DM events) selecting the exposure which leads to 1 CEνNS count. Then, varying over the energy threshold E_R^{thr}, we keep the value which minimizes the cross-section. By repeating such a procedure for a dense grid of WIMP masses in the range [1, 1000] GeV, we

construct the contours shown in Fig. 4. The black upper border of the yellow region corresponds to the ordinary floor. The upper edge of the other colored regions refers to the case of PBHs with parameters in the legend, where for the sake of clarity, we use the same values and color convention adopted in Figs. 1 and 2.

Here, an important remark is in order. For sufficiently high PBH masses $M_{\text{PBH}} \gtrsim 10^{21}$g $\sim 10^{-12} M_\odot$ ($M_\odot$ being the solar mass), the existence of WIMPs as a dominant or subdominant component of DM, is incompatible even with a small fraction of DM made of PBHs [106–114]. This occurs because WIMPs are accreted by the PBH potential well, forming spiked ultra-compact mini-halos, whose existence can be excluded by the non-observation of the expected products of WIMPs self-annihilation. However, for the low PBHs masses considered in our work, falling in the so-called evaporation range ($M_{\text{PBH}} \lesssim 10^{16}$g $\sim 10^{-17} M_\odot$), this phenomenon is negligible. In addition, one should note that DM may be asymmetric [115–117], and this may occur also for WIMPs [118], in which case self-annihilation is suppressed (albeit not necessarily absent [119–122]). Therefore, we deem it interesting to consider how the neutrino floor is modified by the presence of a minute DM fraction of PBHs with mass in the range considered in this work.

6. Conclusions

We have explored a new avenue in constraining PBHs as Dark Matter with the neutrinos emitted in the Hawking radiation. Specifically, we have pointed out that neutrinos from PBHs can interact via the coherent elastic neutrino nucleus scattering (CEνNS) in multi-ton DM direct detection experiments. We have shown that with the high exposures envisaged for the next-generation facilities, it will be possible to set bounds on the fraction of DM composed of PBHs, improving the existing neutrino limits obtained with SK. In addition, we have quantified how much a signal originating from PBHs would heighten the so-called "neutrino floor". While we have focused our study on liquid xenon detectors such as DARWIN [123], LZ [124], and XENONnT [125], other targets such as liquid argon employed in DarkSide-20k [84] and ARGO [84], or archeological lead in RES-NOVA [126], should offer a similar opportunity provided that very high exposures are reached (see [127] for an extensive review of the experimental program of the direct detection facilities). Finally, we underline that, in the context of PBHs searches, the *direct* DM experiments would rather operate as *indirect* DM observatories. From this perspective, our study lends further support to the emerging role of such underground facilities as multi-purpose low-energy neutrino telescopes complementary to their high-energy "ordinary" counterparts, IceCube and KM3NeT.

Declaration of competing interest

The authors declare that they have no known competing financial interests or personal relationships that could have appeared to influence the work reported in this paper.

Acknowledgements

References

[1] R. Abbott, et al., LIGO Scientific, Virgo, GW190521: a binary black hole merger with a total mass of $150M_\odot$, Phys. Rev. Lett. 125 (2020) 101102, arXiv:2009.01075.

[2] B.P. Abbott, et al., LIGO Scientific, Virgo, Binary black hole population properties inferred from the first and second observing runs of advanced LIGO and advanced Virgo, Astrophys. J. Lett. 882 (2019) L24, arXiv:1811.12940.

[3] S. Bird, I. Cholis, J.B. Muñoz, Y. Ali-Haïmoud, M. Kamionkowski, E.D. Kovetz, A. Raccanelli, A.G. Riess, Did LIGO detect dark matter?, Phys. Rev. Lett. 116 (2016) 201301, arXiv:1603.00464.

[4] S. Clesse, J. García-Bellido, The clustering of massive primordial black holes as dark matter: measuring their mass distribution with advanced LIGO, Phys. Dark Universe 15 (2017) 142, arXiv:1603.05234.

[5] M. Sasaki, T. Suyama, T. Tanaka, S. Yokoyama, Primordial black hole scenario for the gravitational-wave event GW150914, Phys. Rev. Lett. 117 (2016) 061101, Erratum: Phys. Rev. Lett. 121 (2018) 059901, arXiv:1603.08338.

[6] S. Blinnikov, A. Dolgov, N.K. Porayko, K. Postnov, Solving puzzles of GW150914 by primordial black holes, J. Cosmol. Astropart. Phys. 11 (2016) 036, arXiv:1611.00541.

[7] T. Nakama, J. Silk, M. Kamionkowski, Stochastic gravitational waves associated with the formation of primordial black holes, Phys. Rev. D 95 (2017) 043511, arXiv:1612.06264.

[8] Y.B. Zel'dovich, I.D. Novikov, The hypothesis of cores retarded during expansion and the hot cosmological model, Sov. Astron., A.J. (Engl. Transl.) 10 (1967) 602.

[9] S. Hawking, Gravitationally collapsed objects of very low mass, Mon. Not. R. Astron. Soc. 152 (1971) 75.

[10] B.J. Carr, S.W. Hawking, Black holes in the early Universe, Mon. Not. R. Astron. Soc. 168 (1974) 399.

[11] S.W. Hawking, Black hole explosions, Nature 248 (1974) 30.

[12] B.J. Carr, The primordial black hole mass spectrum, Astrophys. J. 201 (1975) 1.

[13] G.F. Chapline, Cosmological effects of primordial black holes, Nature 253 (1975) 251.

[14] M. Khlopov, B.A. Malomed, I.B. Zeldovich, Gravitational instability of scalar fields and formation of primordial black holes, Mon. Not. R. Astron. Soc. 215 (1985) 575.

[15] M. Sasaki, T. Suyama, T. Tanaka, S. Yokoyama, Primordial black holes—perspectives in gravitational wave astronomy, Class. Quantum Gravity 35 (2018) 063001, arXiv:1801.05235.

[16] B. Carr, K. Kohri, Y. Sendouda, J. Yokoyama, Constraints on primordial black holes, arXiv:2002.12778, 2020.

[17] A.M. Green, B.J. Kavanagh, Primordial black holes as a dark matter candidate, J. Phys. G 48 (2021) 4, arXiv:2007.10722.

[18] B. Carr, F. Kuhnel, Primordial black holes as dark matter: recent developments, Annu. Rev. Nucl. Part. Sci. 70 (2020) 355, arXiv:2006.02838.

[19] P. Villanueva-Domingo, O. Mena, S. Palomares-Ruiz, A brief review on primordial black holes as dark matter, arXiv:2103.12087, 2021.

[20] S.W. Hawking, Particle creation by black holes, Commun. Math. Phys. 43 (1975) 199, Erratum: Commun. Math. Phys. 46 (1976) 206.

[21] G. Ballesteros, J. Coronado-Blázquez, D. Gaggero, X-ray and gamma-ray limits on the primordial black hole abundance from Hawking radiation, Phys. Lett. B 808 (2020) 135624, arXiv:1906.10113.

[22] J. Iguaz, P.D. Serpico, T. Siegert, Isotropic X-ray bound on primordial black hole dark matter, arXiv:2104.03145, 2021.

[23] B.J. Carr, K. Kohri, Y. Sendouda, J. Yokoyama, Constraints on primordial black holes from the Galactic gamma-ray background, Phys. Rev. D 94 (2016) 044029, arXiv:1604.05349.

[24] A. Arbey, J. Auffinger, J. Silk, Constraining primordial black hole masses with the isotropic gamma ray background, Phys. Rev. D 101 (2020) 023010, arXiv:1906.04750.

[25] R. Laha, J.B. Muñoz, T.R. Slatyer, INTEGRAL constraints on primordial black holes and particle dark matter, Phys. Rev. D 101 (2020) 123514, arXiv:2004.00627.

[26] A. Coogan, L. Morrison, S. Profumo, Direct detection of Hawking radiation from asteroid-mass primordial black holes, Phys. Rev. Lett. 126 (2021) 171101, arXiv:2010.04797.

[27] A. Ray, R. Laha, J.B. Muñoz, R. Caputo, Closing the gap: near future MeV telescopes can discover asteroid-mass primordial black hole dark matter, arXiv:2102.06714, 2021.

[28] R. Laha, Primordial black holes as a dark matter candidate are severely constrained by the Galactic center 511 keV γ-ray line, Phys. Rev. Lett. 123 (2019) 251101, arXiv:1906.09994.

[29] B. Dasgupta, R. Laha, A. Ray, Neutrino and positron constraints on spinning primordial black hole dark matter, Phys. Rev. Lett. 125 (2020) 101101, arXiv:1912.01014.

[30] C. Keith, D. Hooper, The 511 keV excess and primordial black holes in our Solar System, arXiv:2103.08611, 2021.

[31] M. Boudaud, M. Cirelli, Voyager 1 $e^\pm$ further constrain primordial black holes as dark matter, Phys. Rev. Lett. 122 (2019) 041104, arXiv:1807.03075.

[32] V. Poulin, J. Lesgourgues, P.D. Serpico, Cosmological constraints on exotic injection of electromagnetic energy, J. Cosmol. Astropart. Phys. 03 (2017) 043, arXiv:1610.10051.

[33] S. Clark, B. Dutta, Y. Gao, L.E. Strigari, S. Watson, Planck constraint on relic primordial black holes, Phys. Rev. D 95 (2017) 083006, arXiv:1612.07738.

[34] H. Poulter, Y. Ali-Haïmoud, J. Hamann, M. White, A.G. Williams, CMB constraints on ultra-light primordial black holes with extended mass distributions, arXiv:1907.06485, 2019.

[35] B. Dutta, A. Kar, L.E. Strigari, Constraints on MeV dark matter and primordial black holes: inverse compton signals at the SKA, J. Cosmol. Astropart. Phys. 03 (2021) 011, arXiv:2010.05977.

[36] M.H. Chan, C.M. Lee, Constraining primordial black hole fraction at the Galactic centre using radio observational data, Mon. Not. R. Astron. Soc. 497 (2020) 1212, arXiv:2007.05677.

[37] A. Halder, S. Banerjee, Bounds on abundance of primordial black hole and dark matter from EDGES 21-cm signal, Phys. Rev. D 103 (2021) 063044, arXiv:2102.00959.

[38] R. Laha, P. Lu, V. Takhistov, Gas heating from spinning and non-spinning evaporating primordial black holes, arXiv:2009.11837, 2020.

[39] H. Kim, A constraint on light primordial black holes from the interstellar medium temperature, arXiv:2007.07739, 2020.

[40] F. Halzen, B. Keszthelyi, E. Zas, Neutrinos from primordial black holes, Phys. Rev. D 52 (1995) 3239, arXiv:hep-ph/9502268.

[41] E.V. Bugaev, K.V. Konishchev, Constraints on diffuse neutrino background from primordial black holes, Phys. Rev. D 65 (2002) 123005, arXiv:astro-ph/0005295.

[42] E.V. Bugaev, K.V. Konishchev, Cosmological constraints from evaporations of primordial black holes, Phys. Rev. D 66 (2002) 084004, arXiv:astro-ph/0206082.

[43] K. Bays, et al., Super-Kamiokande, Supernova relic neutrino search at Super-Kamiokande, Phys. Rev. D 85 (2012) 052007, arXiv:1111.5031.

[44] S. Wang, D.-M. Xia, X. Zhang, S. Zhou, Z. Chang, Constraining primordial black holes as dark matter at JUNO, Phys. Rev. D 103 (2021) 043010, arXiv:2010.16053.

[45] D.Z. Freedman, Coherent neutrino nucleus scattering as a probe of the weak neutral current, Phys. Rev. D 9 (1974) 1389.

[46] D. Akimov, et al., COHERENT, Observation of coherent elastic neutrino-nucleus scattering, Science 357 (2017) 1123, arXiv:1708.01294.

[47] B. Cabrera, L.M. Krauss, F. Wilczek, Bolometric detection of neutrinos, Phys. Rev. Lett. 55 (1985) 25.

[48] A.K. Drukier, K. Freese, D.N. Spergel, Detecting cold dark matter candidates, Phys. Rev. D 33 (1986) 3495.

[49] J. Monroe, P. Fisher, Neutrino backgrounds to dark matter searches, Phys. Rev. D 76 (2007) 033007, arXiv:0706.3019.

[50] J.D. Vergados, H. Ejiri, Can solar neutrinos be a serious background in direct dark matter searches?, Nucl. Phys. B 804 (2008) 144, arXiv:0805.2583.

[51] L.E. Strigari, Neutrino coherent scattering rates at direct dark matter detectors, New J. Phys. 11 (2009) 105011, arXiv:0903.3630.

[52] A. Gutlein, et al., Solar and atmospheric neutrinos: background sources for the direct dark matter search, Astropart. Phys. 34 (2010) 90, arXiv:1003.5530.

[53] J. Billard, L. Strigari, E. Figueroa-Feliciano, Implication of neutrino backgrounds on the reach of next generation dark matter direct detection experiments, Phys. Rev. D 89 (2014) 023524, arXiv:1307.5458.

[54] D.N. Page, Particle emission rates from a black hole: massless particles from an uncharged, nonrotating hole, Phys. Rev. D 13 (1976) 198.

[55] D.N. Page, Particle emission rates from a black hole. 3. Charged leptons from a nonrotating hole, Phys. Rev. D 16 (1977) 2402.

[56] J.H. MacGibbon, B.R. Webber, Quark and gluon jet emission from primordial black holes: the instantaneous spectra, Phys. Rev. D 41 (1990) 3052.

[57] A. Arbey, J. Auffinger, BlackHawk: a public code for calculating the Hawking evaporation spectra of any black hole distribution, Eur. Phys. J. C 79 (2019) 693, arXiv:1905.04268.

[58] C. Lunardini, Y.F. Perez-Gonzalez, Dirac and Majorana neutrino signatures of primordial black holes, J. Cosmol. Astropart. Phys. 08 (2020) 014, arXiv:1910.07864.

[59] D. Hooper, G. Krnjaic, S.D. McDermott, Dark radiation and superheavy dark matter from black hole domination, J. High Energy Phys. 08 (2019) 001, arXiv:1905.01301.

[60] I. Masina, Dark matter and dark radiation from evaporating primordial black holes, Eur. Phys. J. Plus 135 (2020) 552, arXiv:2004.04740.

[61] J.F. Navarro, C.S. Frenk, S.D.M. White, A Universal density profile from hierarchical clustering, Astrophys. J. 490 (1997) 493, arXiv:astro-ph/9611107.

[62] P. Salucci, F. Nesti, G. Gentile, C.F. Martins, The dark matter density at the Sun's location, Astron. Astrophys. 523 (2010) A83, arXiv:1003.3101.

[63] M. Pato, F. Iocco, G. Bertone, Dynamical constraints on the dark matter distribution in the Milky Way, J. Cosmol. Astropart. Phys. 12 (2015) 001, arXiv:1504.06324.

[64] M. Benito, A. Cuoco, F. Iocco, Handling the uncertainties in the Galactic dark matter distribution for particle dark matter searches, J. Cosmol. Astropart. Phys. 03 (2019) 033, arXiv:1901.02460.

[65] E.V. Karukes, M. Benito, F. Iocco, R. Trotta, A. Geringer-Sameth, Bayesian reconstruction of the Milky Way dark matter distribution, J. Cosmol. Astropart. Phys. 09 (2019) 046, arXiv:1901.02463.

[66] P.F. de Salas, K. Malhan, K. Freese, K. Hattori, M. Valluri, On the estimation of the local dark matter density using the rotation curve of the Milky Way, J. Cosmol. Astropart. Phys. 10 (2019) 037, arXiv:1906.06133.

[67] P.F. de Salas, A. Widmark, Dark matter local density determination: recent observations and future prospects, arXiv:2012.11477, 2020.

[68] F. Nesti, P. Salucci, The dark matter halo of the Milky Way, AD 2013, J. Cosmol. Astropart. Phys. 07 (2013) 016, arXiv:1304.5127.

[69] N. Aghanim, et al., Planck, Planck 2018 results. VI. Cosmological parameters, Astron. Astrophys. 641 (2020) A6, arXiv:1807.06209.

[70] N. Vinyoles, A.M. Serenelli, F.L. Villante, S. Basu, J. Bergström, M.C. Gonzalez-Garcia, M. Maltoni, C. Peña Garay, N. Song, A new generation of standard solar models, Astrophys. J. 835 (2017) 202, arXiv:1611.09867.

[71] J.F. Beacom, The diffuse supernova neutrino background, Annu. Rev. Nucl. Part. Sci. 60 (2010) 439, arXiv:1004.3311.

[72] G. Battistoni, A. Ferrari, T. Montaruli, P.R. Sala, The atmospheric neutrino flux below 100-MeV: the FLUKA results, Astropart. Phys. 23 (2005) 526.

[73] M. Honda, T. Kajita, K. Kasahara, S. Midorikawa, Improvement of low energy atmospheric neutrino flux calculation using the JAM nuclear interaction model, Phys. Rev. D 83 (2011) 123001, arXiv:1102.2688.

[74] K. Kohri, J. Yokoyama, Primordial black holes and primordial nucleosynthesis. 1. Effects of hadron injection from low mass holes, Phys. Rev. D 61 (2000) 023501, arXiv:astro-ph/9908160.

[75] J.H. MacGibbon, B.J. Carr, D.N. Page, Do evaporating black holes form photospheres?, Phys. Rev. D 78 (2008) 064043, arXiv:0709.2380.

[76] C. Patrignani, et al., Particle Data Group, Review of particle physics, Chin. Phys. C 40 (2016) 100001.

[77] R.H. Helm, Inelastic and elastic scattering of 187-Mev electrons from selected even-even nuclei, Phys. Rev. 104 (1956) 1466.

[78] J.D. Lewin, P.F. Smith, Review of mathematics, numerical factors, and corrections for dark matter experiments based on elastic nuclear recoil, Astropart. Phys. 6 (1996) 87.

[79] J.L. Newstead, R.F. Lang, L.E. Strigari, Atmospheric neutrinos in a next-generation xenon dark matter experiment, arXiv:2002.08566, 2020.

[80] A. Priya, C. Lunardini, Diffuse neutrinos from luminous and dark supernovae: prospects for upcoming detectors at the $O(10)$ kt scale, J. Cosmol. Astropart. Phys. 11 (2017) 031, arXiv:1705.02122.

[81] S. Horiuchi, K. Sumiyoshi, K. Nakamura, T. Fischer, A. Summa, T. Takiwaki, H.-T. Janka, K. Kotake, Diffuse supernova neutrino background from extensive core-collapse simulations of 8-100M$_\odot$ progenitors, Mon. Not. R. Astron. Soc. 475 (2018) 1363, arXiv:1709.06567.

[82] K. Møller, A.M. Suliga, I. Tamborra, P.B. Denton, Measuring the supernova unknowns at the next-generation neutrino telescopes through the diffuse neutrino background, J. Cosmol. Astropart. Phys. 05 (2018) 066, arXiv:1804.03157.

[83] D. Kresse, T. Ertl, H.-T. Janka, Stellar collapse diversity and the diffuse supernova neutrino background, Astrophys. J. 909 (2021) 169, arXiv:2010.04728.

[84] C.E. Aalseth, et al., DarkSide-20k, DarkSide-20k: a 20 tonne two-phase LAr TPC for direct dark matter detection at LNGS, Eur. Phys. J. Plus 133 (2018) 131, arXiv:1707.08145.

[85] J.B. Dent, B. Dutta, J.L. Newstead, L.E. Strigari, Effective field theory treatment of the neutrino background in direct dark matter detection experiments, Phys. Rev. D 93 (2016) 075018, arXiv:1602.05300.

[86] G.B. Gelmini, V. Takhistov, S.J. Witte, Casting a wide signal net with future direct dark matter detection experiments, J. Cosmol. Astropart. Phys. 07 (2018) 009, Erratum: J. Cosmol. Astropart. Phys. 02 (2019) E02, arXiv:1804.01638.

[87] E. Aprile, et al., XENON, Search for coherent elastic scattering of Solar ^{8}B neutrinos in the XENON1T dark matter experiment, Phys. Rev. Lett. 126 (2021) 091301, arXiv:2012.02846.

[88] J.H. Davis, Dark matter vs. neutrinos: the effect of astrophysical uncertainties and timing information on the neutrino floor, J. Cosmol. Astropart. Phys. 03 (2015) 012, arXiv:1412.1475.

[89] F. Ruppin, J. Billard, E. Figueroa-Feliciano, L. Strigari, Complementarity of dark matter detectors in light of the neutrino background, Phys. Rev. D 90 (2014) 083510, arXiv:1408.3581.

[90] P. Grothaus, M. Fairbairn, J. Monroe, Directional dark matter detection beyond the neutrino bound, Phys. Rev. D 90 (2014) 055018, arXiv:1406.5047.

[91] C.A.J. O'Hare, A.M. Green, J. Billard, E. Figueroa-Feliciano, L.E. Strigari, Readout strategies for directional dark matter detection beyond the neutrino background, Phys. Rev. D 92 (2015) 063518, arXiv:1505.08061.

[92] C.A.J. O'Hare, Can we overcome the neutrino floor at high masses?, Phys. Rev. D 102 (2020) 063024, arXiv:2002.07499.

[93] R. Harnik, J. Kopp, P.A.N. Machado, Exploring nu signals in dark matter detectors, J. Cosmol. Astropart. Phys. 07 (2012) 026, arXiv:1202.6073.

[94] D.G. Cerdeño, M. Fairbairn, T. Jubb, P.A.N. Machado, A.C. Vincent, C. Bœhm, Physics from solar neutrinos in dark matter direct detection experiments, J. High Energy Phys. 05 (2016) 118, Erratum: J. High Energy Phys. 09 (2016) 048, arXiv:1604.01025.

[95] D.K. Papoulias, R. Sahu, T.S. Kosmas, V.K.B. Kota, B. Nayak, Novel neutrino-floor and dark matter searches with deformed shell model calculations, Adv. High Energy Phys. 2018 (2018) 6031362, arXiv:1804.11319.

[96] A.M. Suliga, I. Tamborra, Astrophysical constraints on nonstandard coherent neutrino-nucleus scattering, Phys. Rev. D 103 (2021) 083002, arXiv:2010.14545.

[97] J.B. Dent, B. Dutta, J.L. Newstead, L.E. Strigari, Dark matter, light mediators, and the neutrino floor, Phys. Rev. D 95 (2017) 051701, arXiv:1607.01468.

[98] E. Bertuzzo, F.F. Deppisch, S. Kulkarni, Y.F. Perez Gonzalez, R. Zukanovich Funchal, Dark matter and exotic neutrino interactions in direct detection searches, J. High Energy Phys. 04 (2017) 073, arXiv:1701.07443.

[99] M.C. Gonzalez-Garcia, M. Maltoni, Y.F. Perez-Gonzalez, R. Zukanovich Funchal, Neutrino discovery limit of dark matter direct detection experiments in the presence of non-standard interactions, J. High Energy Phys. 07 (2018) 019, arXiv:1803.03650.

[100] C. Bœhm, D.G. Cerdeño, P.A.N. Machado, A. Olivares-Del Campo, E. Perdomo, E. Reid, How high is the neutrino floor?, J. Cosmol. Astropart. Phys. 01 (2019) 043, arXiv:1809.06385.

[101] W. Chao, J.-G. Jiang, X. Wang, X.-Y. Zhang, Direct detections of dark matter in the presence of non-standard neutrino interactions, J. Cosmol. Astropart. Phys. 08 (2019) 010, arXiv:1904.11214.

[102] S. Sadhukhan, M.P. Singh, Neutrino floor in leptophilic $U(1)$ models: modification in $U(1)_{L_\mu - L_\tau}$, Phys. Rev. D 103 (2021) 015015, arXiv:2006.05981.

[103] Y. Cui, M. Pospelov, J. Pradler, Signatures of dark radiation in neutrino and dark matter detectors, Phys. Rev. D 97 (2018) 103004, arXiv:1711.04531.

[104] M. Nikolic, S. Kulkarni, J. Pradler, The neutrino-floor in the presence of dark radiation, arXiv:2008.13557, 2020.

[105] V. Munoz, V. Takhistov, S.J. Witte, G.M. Fuller, Exploring the origin of supermassive black holes with coherent neutrino scattering, arXiv:2102.00885, 2021.

[106] B.C. Lacki, J.F. Beacom, Primordial black holes as dark matter: almost all or almost nothing, Astrophys. J. Lett. 720 (2010) L67, arXiv:1003.3466.

[107] S.M. Boucenna, F. Kuhnel, T. Ohlsson, L. Visinelli, Novel constraints on mixed dark-matter scenarios of primordial black holes and WIMPs, J. Cosmol. Astropart. Phys. 07 (2018) 003, arXiv:1712.06383.

[108] J. Adamek, C.T. Byrnes, M. Gosenca, S. Hotchkiss, WIMPs and stellar-mass primordial black holes are incompatible, Phys. Rev. D 100 (2019) 023506, arXiv:1901.08528.

[109] G. Bertone, A.M. Coogan, D. Gaggero, B.J. Kavanagh, C. Weniger, Primordial black holes as silver bullets for new physics at the weak scale, Phys. Rev. D 100 (2019) 123013, arXiv:1905.01238.

[110] R.-G. Cai, Y.-C. Ding, X.-Y. Yang, Y.-F. Zhou, Constraints on a mixed model of dark matter particles and primordial black holes from the galactic 511 keV line, J. Cosmol. Astropart. Phys. 03 (2021) 057, arXiv:2007.11804.

[111] B. Carr, F. Kuhnel, L. Visinelli, Black holes and WIMPs: all or nothing or something else, arXiv:2011.01930, 2020.

[112] M.P. Hertzberg, S. Nurmi, E.D. Schiappacasse, T.T. Yanagida, Shining primordial black holes, Phys. Rev. D 103 (2021) 063025, arXiv:2011.05922.

[113] K. Kadota, J. Silk, Boosting small-scale structure via primordial black holes and implications for sub-GeV dark matter annihilation, Phys. Rev. D 103 (2021) 043530, arXiv:2012.03698.

[114] H. Tashiro, K. Kadota, Constraining mixed dark-matter scenarios of WIMPs and primordial black holes from CMB and 21-cm observations, arXiv:2104.09738, 2021.

[115] D.E. Kaplan, M.A. Luty, K.M. Zurek, Asymmetric dark matter, Phys. Rev. D 79 (2009) 115016, arXiv:0901.4117.

[116] K. Petraki, R.R. Volkas, Review of asymmetric dark matter, Int. J. Mod. Phys. A 28 (2013) 1330028, arXiv:1305.4939.

[117] K.M. Zurek, Asymmetric dark matter: theories, signatures, and constraints, Phys. Rep. 537 (2014) 91, arXiv:1308.0338.

[118] M.L. Graesser, I.M. Shoemaker, L. Vecchi, Asymmetric WIMP dark matter, J. High Energy Phys. 10 (2011) 110, arXiv:1103.2771.

[119] T. Cohen, K.M. Zurek, Leptophilic dark matter from the lepton asymmetry, Phys. Rev. Lett. 104 (2010) 101301, arXiv:0909.2035.

[120] Y. Cai, M.A. Luty, D.E. Kaplan, Leptonic indirect detection signals from strongly interacting asymmetric dark matter, arXiv:0909.5499, 2009.

[121] I. Baldes, K. Petraki, Asymmetric thermal-relic dark matter: Sommerfeld-enhanced freeze-out, annihilation signals and unitarity bounds, J. Cosmol. Astropart. Phys. 09 (2017) 028, arXiv:1703.00478.

[122] I. Baldes, M. Cirelli, P. Panci, K. Petraki, F. Sala, M. Taoso, Asymmetric dark matter: residual annihilations and self-interactions, SciPost Phys. 4 (2018) 041, arXiv:1712.07489.

[123] J. Aalbers, et al., DARWIN, DARWIN: towards the ultimate dark matter detector, J. Cosmol. Astropart. Phys. 11 (2016) 017, arXiv:1606.07001.

[124] D.S. Akerib, et al., LUX-ZEPLIN, Projected WIMP sensitivity of the LUX-ZEPLIN dark matter experiment, Phys. Rev. D 101 (2020) 052002, arXiv:1802.06039.

[125] E. Aprile, et al., XENON, Projected WIMP sensitivity of the XENONnT dark matter experiment, J. Cosmol. Astropart. Phys. 11 (2020) 031, arXiv:2007.08796.

[126] L. Pattavina, N. Ferreiro Iachellini, I. Tamborra, Neutrino observatory based on archaeological lead, Phys. Rev. D 102 (2020) 063001, arXiv:2004.06936.

[127] J. Billard, et al., Direct detection of dark matter – APPEC committee report, arXiv:2104.07634, 2021.